On the Coexistence of LoRa- and Interleaved Chirp Spreading LoRa-Based Modulations

Phoebe Edward*, Sondos Elzeiny†, Mohamed Ashour‡, & Tallal Elshabrawy§
Faculty of Information Engineering & Technology, the German University in Cairo, Egypt
Email: {*phoebe.edward, †sondos.elzeiny@student, ‡mohamed.ashour, §tallal.el-shabrawy}@guc.edu.eg

***Abstract*—LoRa has recently established itself as one of the leading low power wide area networks (LP-WAN) technologies. LoRa modulation is a chirp spread spectrum-based modulation. Cyclic shifts of a linearly increasing chirp signal constitute a multi-dimensional space for nominal LoRa communication. LoRa networks are typically capacity-limited due to the adopted ALOHA-based medium access scheme. One approach to enhance the network capacity could be by introducing new LoRa-based communication channels that exhibit good cross-correlation properties with respect to the nominal LoRa chirp signals. In our recent work, Interleaved Chirp Spreading LoRa (ICS-LoRa) has been introduced as a new multi-dimensional space generated from interleaved versions of the nominal LoRa chirp signals. ICS-LoRa capable transmitters have used the extended multi-dimensional space to introduce one additional bit within each transmitted chirp signal. In this paper, we investigate the possibility of deploying ICS-LoRa to rather create a new overlapping logical network that co-exists with the nominal LoRa network. This would have the potential of increasing the overall system capacity by up to 100%. Accordingly, we specifically focus on studying the inter-network interference between the nominal LoRa and the ICS-LoRa logical networks at different Signal to Interference Ratio (SIR) and at different Signal to Noise Ratio (SNR) scenarios. Simulation results indicate that ICS-LoRa interference has mild effects on the BER performance of nominal LoRa demodulation and vice versa. Moreover, we demonstrate that the favorable cross-correlation characteristics create a better chance for successful interference cancellation of inter-network interfering signals. This opens further room for enhancing the overall system capacity.**

***Index Terms*—LP-WAN, LoRa Modulation, ICS-LoRa Modulation, BER Performance Analysis, Interference Cancellation, LoRa Capacity.**

I. Introduction

The last few years have witnessed rapid innovations in the field of Internet of Things (IoT). LoRa has established itself as one of the front runners among low power wide area networks (LP-WAN) serving as the key infrastructure to support numerous IoT applications. The number of countries deploying LoRa-based solutions has been fast growing and it is now approaching 150 countries (currently standing at 142 countries [1]). LoRa modulation is mainly pillared on its chirp spread spectrum communication where the rate of frequency increase of each chirp signal depends on the applied spreading factor. LoRa supports long-range communication (at the scale of kilometers) between multiple end-devices (ED) and a supporting gateway to relay LoRa data towards cloud servers. The adopted medium access scheme within LoRa networks is the ALOHA medium access scheme. Consequently, LoRa signals suffer from inevitable collisions that limit the capacity of the whole network. However, LoRa signals with different spreading factors are quasi-orthogonal [1], thus multiple simultaneous logical LoRa networks can co-exist. On the other hand, the co-existence of LoRa signals with the same spreading factor still suffers from the effect of collisions, and this is the main challenge that is tackled in this paper.

Numerous research have addressed the issue of intra-network same spreading factor interference [1–4]. Among these techniques are: the capture effect (CE) [1, 5–7] and the successive interference cancellation (SIC) [7]. In CE technique, the receiver decodes only the strongest received signal. On the other hand, in the SIC, the receiver attempts to decode all the received signals in order of their received power. In SIC, the receiver iteratively reconstructs the decoded signal to subtract it from the aggregate received signal. Both the CE and SIC require that the signal to interference ratio (SIR) of the desired signal to be decoded should be greater than some threshold value [1–4]. Decoding superposed LoRa signals of similar received power is not possible through CE and SIC [8]. In [9], the timing information has been used to link the received signal to the correct ED transmitter and to decode it. However, they have some limitations in their proposed technique. In [10], a combination of chirp spread spectrum (CSS) modulation and ON-OFF keying have been deployed to enable large scale of concurrent transmissions from hundreds of back-scatter ED. Nevertheless, each ED is allowed to send only one bit within the duration of the whole symbol, thus a huge degradation is witnessed in the ED data rate. All these previous techniques have been confined within the scope of nominal LoRa signals. To the best of the authors' knowledge, the possibility of enhancing system capacity by extending the number of dimensions for more communication channels has not been investigated.

In our recent work in [11], Interleaved Chirp Spreading LoRa (ICS-LoRa) has been introduced as a new multi-dimensional space for LoRa-based signaling. ICS-LoRa chirps have been shown to exhibit good cross-correlation with respect to the nominal LoRa chirp signals. ICS-LoRa chirps have been simply generated by sub-dividing each nominal LoRa chirp into four sub-intervals and interleaving these sub-intervals by a certain interleaving pattern. ICS-LoRa capable transmitters have been then used to extend multi-dimensional space for communication and introduce one additional bit within each transmitted chirp signal for a gain of up to 14% in user data rates [11]. In this paper, we investigate the possibility

[1] https://www.lora-alliance.org

978-1-7281-3316-4/19/$31.00 ©2019 IEEE

of deploying ICS-LoRa to rather create a new overlapping logical network that co-exists with the nominal LoRa network. Accordingly, the inter-network interference effect between ICS-LoRa and nominal LoRa logical networks are studied. The inter-network interference is also compared against the intra-network interference associated with concurrent nominal LoRa signal transmissions. Simulation results indicate that ICS-LoRa interference has mild effects on the BER performance of nominal LoRa demodulation and vice versa. Therefore, under the scenarios of inter-network interference between nominal LoRa and ICS-LoRa signals, the network gateway has a great chance to capture the stronger signal and apply interference cancellation to decode both the stronger and weaker signals, respectively.

The rest of this paper is organized as follows: Overview of nominal LoRa modulation and demodulation as well as the Interleaved Chirp Spreading LoRa (ICS-LoRa) modulation and demodulation are all reviewed in Section II. In Section III, the co-existence of the ICS-LoRa logical network with the nominal LoRa network is investigated. A comparison between the inter-network interference and the intra-network interference effects is demonstrated through the simulation results within Section IV. Finally, Section V is dedicated for conclusions.

II. Overview of LoRa- and ICS-LoRa- Based Modulations

A. Nominal LoRa Modulation and Demodulation

In the nominal LoRa modulation, non-binary LoRa symbols could be represented in terms of discrete cyclic frequency shifts of some base CSS discrete-time signal $\omega_0(nT)$ that is given as

$$\omega_0(nT) = \sqrt{\frac{1}{2^f}} \exp\left[j2\pi \cdot \frac{(nT)^2}{2} \cdot \frac{B}{T_S}\right], \quad (1)$$

where B is the LoRa bandwidth, $T = 1/B$ is the sample interval, $n = 0, 1, 2, \ldots, 2^f - 1$ depicts the sample index at time $t = nT$ and f is the LoRa modulation spreading factor that governs the symbol duration T_S to be comprised of 2^f samples such that $T_S = 2^f \cdot T$. Accordingly, the base chirp signal $\omega_0(nT)$ in (1) could be simplified as

$$\omega_0(n) = \sqrt{\frac{1}{2^f}} \exp\left[j2\pi \cdot \frac{n^2}{2^{f+1}}\right]. \quad (2)$$

As presented in [11], nominal LoRa modulation could be realized through the deployment of 2^f cyclic time-shifts of the base chirp signal $\omega_0(n)$ in order to represent 2^f distinct non-binary LoRa symbols $\Omega_m = m$, $m \in M = \{0, 1, 2, \ldots, 2^f - 1\}$. Accordingly, let us define $\omega_m(n)$, $m \in M = \{0, 1, 2, \ldots, 2^f - 1\}$ as a LoRa chirp signal generated from the m^{th} cyclic time-shift of $\omega_0(n)$ such that $\omega_m(n)$ is expressed as

$$\omega_m(n) = \sqrt{\frac{1}{2^f}} \exp\left[j2\pi \cdot \frac{\left((m+n) \mod 2^f\right)^2}{2^{f+1}}\right]. \quad (3)$$

Considering a nominal LoRa chirp signal that passed through AWGN channel, the LoRa receiver possesses two steps for decoding; the dechirping and the DFT. Dechirping is achieved by correlating the received chirp with the base chirp signal $\omega_0(n)$ [12], as follows

$$\overline{r}\left(n|\Omega_l\right) = r\left(n|\Omega_l\right) \times \omega_0^*(n), \quad (4)$$

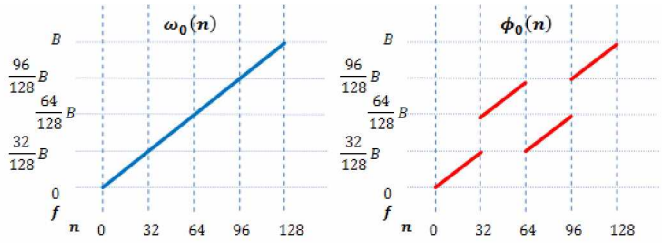

Fig. 1. Illustrative examples for $\omega_0(nT)$ and $\phi_0(nT)$ with $f = 7$.

where $r\left(n|\Omega_l\right)$ denotes the received chirp signal given symbol Ω_l is transmitted, $\overline{r}\left(n|\Omega_l\right)$ is the dechirped received signal, and * denotes complex conjugate.

The DFT is then applied to the resultant samples. As demonstrated in [11], the DFT outputs are given by

$$\mathcal{R}_{k|\Omega_l} = \begin{cases} \sqrt{E_S} + \eta_l & k = l \\ \eta_k & k \neq l \end{cases}, \quad (5)$$

where $\mathcal{R}_{k|\Omega_l}$ is the DFT outputs, given Ω_l symbol is transmitted, E_S is the symbol energy, η_k is the complex Gaussian noise process and k is the DFT outputs index.

Finally, the LoRa detector selects the index of the DFT output that exhibits the highest magnitude [12]. The detected symbol $\hat{l}$, given that the LoRa symbol $\Omega_l = l$ is transmitted, becomes

$$\hat{l} = \arg_k \max\left(\left[\left|\mathcal{R}_{0|\Omega_l}\right|, \ldots, \left|\mathcal{R}_{k|\Omega_l}\right| \ldots, \left|\mathcal{R}_{2^f-1|\Omega_l}\right|\right]\right). \quad (6)$$

In this sub-section, the nominal LoRa modulation and demodulation have been explained. It is to be noted that for convenience of terminology, nominal LoRa shall be referred to as simply LoRa throughout the rest of this paper.

B. ICS-LoRa Modulation and Demodulation

The Interleaved Chirp Spreading LoRa (ICS-LoRa) has been recently introduced in [11] as a new multi-dimensional space for LoRa-based communication. The main motivation behind this ICS-LoRa was to introduce additional chirp signals to support an increase in the number of transmitted bits per chirp signal thus enhancing the capacity per ED. However, in this paper the ICS-LoRa based modulation would be utilized as a standalone modulation scheme for separate ED nodes to co-exist with the ED nodes utilizing the LoRa based modulation.

ICS-LoRa features an ICS interleaver that subdivides the LoRa chirp signal $\omega_q(n)$ composed of 2^f samples into 4 sub-intervals with each sub-interval comprised of $\Delta = 2^{f-2}$ samples. Then, these sub-intervals are interleaved to produce $\phi_q(n)$, as

$$\phi_q(n) = \begin{cases} \omega_q(n) & 0 \leq n < 2^{f-2} \\ \omega_{(q+\Delta) \mod 2^f}(n) & 2^{f-2} \leq n < 2^{f-1} \\ \omega_{(q+3\Delta) \mod 2^f}(n) & 2^{f-1} \leq n < 3 \times 2^{f-2} \\ \omega_q(n) & 3 \times 2^{f-2} \leq n < 2^f \end{cases}. \quad (7)$$

The interleaver function as defined in (7) is applied in ICS-LoRa to each of the LoRa chirp signals $\omega_m(n)$ to generate the corresponding interleaved chirp signal $\phi_m(n)$, $m \in M = \left\{0, 1, \ldots 2^f - 1\right\}$. Figure 1 shows an illustrative example for the LoRa and the interleaved LoRa bases chirp signals $\omega_0(n)$ and $\phi_0(n)$, respectively, with $sf = 7$. It is clear that the ICS interleaver simply swaps the samples of the two middle sub-intervals of $\omega_0(n)$ to generate $\phi_0(n)$. It is also obvious that the

signal $\phi_0(n)$ remains to span the entire available bandwidth B.

In ICS-LoRa, by deploying ICS-interleaving to all 2^f LoRa chirp signals $\omega_m(n)$, it becomes feasible to construct the chirp signals $\phi_m(n)$ that could be used to transmit 2^f non-binary symbols $\Phi_m = m$, $m \in M$.

For demodulation, the received signal first passes through the ICS LoRa de-interleaver. By this de-interleaver, the two middle sub-intervals of the chirp signal $\phi_m(n)$ are re-swaped again to return back to the LoRa chirp signal $\omega_m(n)$. Then the signal follows the same sequence of LoRa demodulation technique where dechirping takes place by multiplying the signal by the complex conjugate of the LoRa basis chirp signal $\omega_0^*(n)$ as in (4). DFT is then applied to the 2^f samples of the dechirped signal. The ICS LoRa symbol detection then reverts to the selection of the DFT output index with the highest magnitude as in (6).

C. LoRa and ICS-LoRa Cross-Correlation

LoRa chirp signals $\omega_m(n)$ are 2^f orthonormal bases functions that are used to represent 2^f non-binary symbols. Similarly, the ICS-LoRa chirp signals $\phi_m(n)$ are also orthonormal bases functions that could be used to represent 2^f non-binary symbols. Since the co-existence of LoRa and ICS-LoRa is studied in this paper, it is important to demonstrate the cross-correlation between the LoRa chirp signals $\omega_m(n)$ and the ICS-LoRa chirp signals $\phi_m(n)$. Figure 2 shows the cross-correlation between the ICS-LoRa chirp signal $\phi_0(n)$ and the LoRa chirp signals for spreading factor $f = 7$. This cross-correlation is generated by dechirping (4) and applying DFT to the 2^f resultant samples. It is obvious from this Figure that the ICS-LoRa chirp signal $\phi_0(n)$ has 50% correlation with the LoRa chirp signal $\omega_0(n)$ since the cross-correlation value is 0.5 at index $k = 0$. Moreover, it has 25% correlation with both the LoRa chirp signals $\omega_{32}(n)$ and $\omega_{96}(n)$ since the cross-correlation value is 0.25 at the indices $k = 32$ and $k = 96$. This is attributed to the fact that the ICS-LoRa chirp signal $\phi_0(n)$ can be alternatively generated by taking the first and last 2^{f-2} samples from the LoRa chirp signal $\omega_0(n)$ and taking the second and third 2^{f-2} samples from the LoRa chirp signals $\omega_{32}(n)$ and $\omega_{96}(n)$ respectively. On the other hand, the cross-correlation of the LoRa chirp signal $\omega_0(n)$ with the LoRa chirp signals result in exactly one peak value of magnitude 1 at index $k = 0$ and a value of zero at all other indices as shown in Figure 2.

For any other ICS-LoRa chirp signal $\phi_l(n)$, it is equivalently generated by taking the first and last 2^{f-2} samples from the LoRa chirp signal $\omega_l(n)$ and taking the second and third 2^{f-2} samples from the LoRa chirp signals $\omega_{(l+\Delta) \mod 2^f}(n)$ and $\omega_{(l+3\Delta) \mod 2^f}(n)$ respectively. Therefore, this ICS-LoRa chirp signal $\phi_l(n)$ will have exactly the same cross-correlation values depicted in Figure 2 but with the correlation values $0.5, 0.25, 0.25$ appearing at indices $k = l$, $k = (l + \Delta) \mod 2^f$ and $k = (l + 3\Delta) \mod 2^f$ respectively. Thus the ICS-LoRa chirp signals are not perfectly orthogonal with the LoRa chirp signals, however they possess good cross-correlation properties. In [11], it was proved that due to the large number of noise values within the DFT outputs of the decoded chirp,

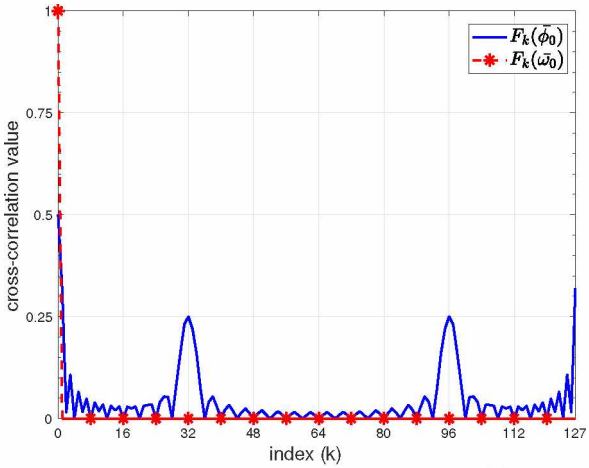

Fig. 2. Cross-Correlation of the ICS-LoRa chirp signal $\phi_0(n)$ and the LoRa chirp signals versus the cross-correlation of the LoRa chirp signal ω_0 with the LoRa chirp signals with $f = 7$.

the system remains to be noise limited when LoRa and ICS-LoRa co-exist. Thus, the loss in performance was proved to be minimal when ICS-LoRa was used to increase one bit. Hence, in this paper, we utilize the ICS-LoRa as a separate logical network that can co-exist with the LoRa network with minimal BER performance loss.

III. System Model

A. System Model of the LoRa Interfered by ICS-LoRa

Let us consider a LoRa basis signal of interest $\omega_l(n)$, that is interfered by some other ICS-LoRa signal that is using the same spreading factor f. Due to desynchronization of the transmitters, a random shift of τ samples occurs between the transmission of the desired signal $\omega_l(n)$ and any interfering signal. Consequently, let us define an interference ICS-LoRa signal $I(q_1, q_2, \tau, n)$ that interferes with $\omega_l(n)$ as

$$I(q_1, q_2, \tau, n) = \begin{cases} \frac{1}{\sqrt{\gamma}}.\phi_{q_1}(n) & 0 \le n < \tau \\ \frac{1}{\sqrt{\gamma}}.\phi_{q_2}(n) & \tau \le n < 2^f \end{cases} \quad (8)$$

where due to the shifts of τ samples between the two transmitters, $\omega_l(n)$ is exposed to interference from two bases ICS signals $\phi_{q_1}(n)$, $\phi_{q_2}(n)$, q_1,$q_2 \in \{0, 1, 2, ..., 2^f - 1\}$ (due to two consecutive interfering ICS-LoRa symbols) during the first τ and last $(2^f - \tau)$ samples of $\omega_l(n)$, respectively[2]. It is assumed that $0 \le \tau \le 2^{f-1}$ such that the number of interfering samples from $\phi_{q_1}(n)$ are smaller or equal to those from $\phi_{q_2}(n)$. It is also assumed that the interference $I(q_1, q_2, \tau, n)$ will result in an SIR γ with respect to the signal of interest $\omega_l(n)$ which has a normalized symbol energy of 1.

Figure 3 shows the system block diagram where there are two ED transmitters; one utilizing LoRa modulator and the other ICS-LoRa modulator. The resulting signals from both transmitters are added together after introducing a delay for the desired LoRa signal by τ samples and multiplying the interferer ICS-LoRa signal by $1/\sqrt{\gamma}$. After that, the aggregate signal of both transmitters passes through the AWGN channel. Thus a combination of the desired LoRa signal, the interferer ICS-LoRa signal and the AWGN arrives at the receiver. Γ is

[2]For the case of $\tau = 0$, $\omega_l(nT)$ will be exposed to only one ICS-LoRa interfering signal $\phi_{z2}(nT)$

the SNR that is experienced by the signal and is related to the signal energy to the noise power spectral density E_s/N_0 using

$$\Gamma = \frac{E_s/T_S}{N_0 \cdot B} = \frac{E_S}{N_0 \cdot 2^f}, \tag{9}$$

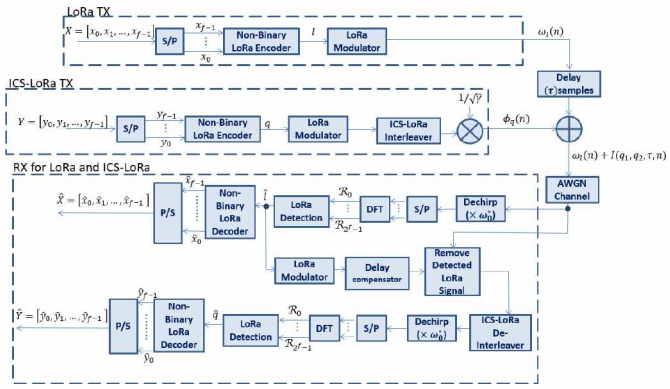

Fig. 3. Block Diagram of LoRa and ICS-LoRa transmitters and one receiver for both

At the receiver gateway node, first the desired LoRa signal is demodulated and detected through dechirping and applying DFT. In order to retrieve the interferer ICS-LoRa signal, the detected LoRa signal is re-modulated once more and then removed from the aggregate received signal by subtraction. However, a delay compensation must be performed to remove the re-modulated LoRa signal correctly from the aggregate received signal. The result of the subtraction is demodulated using ICS-LoRa demodulation technique which starts by the de-interleaver to return the ICS-LoRa chirp signal into the corresponding LoRa chirp signal. In case of intra-network interference of LoRa interfered by LoRa, the ICS-LoRa de-interleaver is not needed. On the other hand, in case of intra-network interference of ICS-LoRa interfered by ICS-LoRa, the ICS-LoRa de-interleaver is required in both demodulation steps.

IV. Simulation Results

A. LoRa Interfered by ICS-LoRa versus ICS-LoRa interfered by LoRa

The system explained in Sub-section III-A has been simulated for two different cases; the first is LoRa interfered by ICS-LoRa signal and the second is ICS-LoRa interfered by LoRa signal. The BER curves of the desired signal in both cases for SIR value $\gamma = 4dB$ and for spreading factors $f = 7, 9, 11$ are shown in Figure 4. The BER values are obtained by averaging the values across all the shift values $\tau = 0, 1, ...2^{f-1}$. It is obvious from the graph that both cases hold exactly the same BER performance. Hence, in the rest of the simulations, only the case of the desired LoRa signal interfered by ICS-LoRa signal will be considered.

B. BER Performance of LoRa Signal with ICS-LoRa Interference

Figures 5, 6, and 7 show the BER performance of the desired LoRa signal in case of ICS-LoRa interference and in case of LoRa interference for spreading factors $f = 7, 9, 11$ respectively. The SIR values used in these simulations are $\gamma = 0, 4, 8dB$. We first notice from the Figures that the BER performance for the different spreading factors $f = 7, 9, 11$

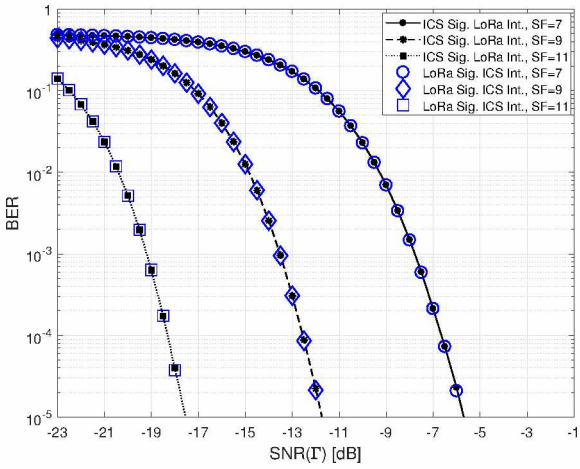

Fig. 4. LoRa interfered by ICS-LoRa versus ICS-LoRa interfered by LoRa, at SIR $\gamma = 4dB$, BER of the desired signal for $f = 7, 9, 11$.

demonstrate similar tendencies. Moreover, since the ICS-LoRa chirp signals have good cross-correlation with respect to the LoRa chirp signals, the interference effect of ICS-LoRa on LoRa signals is low compared to the interference effect of LoRa on LoRa signals. Thus, the impact of ICS-LoRa interference on BER performance is less compared to the LoRa interference. Consequently, the overall system capacity is drastically enhanced. For example, for spreading factor $f = 7$ and SIR value $\gamma = 4dB$, the LoRa signal interfered by ICS-LoRa has a BER degradation of approximately $0.7dB$ compared to approximately $5dB$ in case it is interfered by another LoRa signal. It is also shown that for high SIR values the LoRa signal BER performance approaches the non-interfered signal performance. Another important notice is that for example, for spreading factor $f = 7$, at SIR $\gamma = 0dB$, the LoRa signal interfered by ICS-LoRa can still be decoded at a very good BER performance at SNR (Γ) of approximately $-3dB$, however, the LoRa signal interfered by another LoRa signal at the same SIR $\gamma = 0dB$ can not be successfully decoded at a good BER performance even for high values of SNR (Γ) as illustrated in [8].

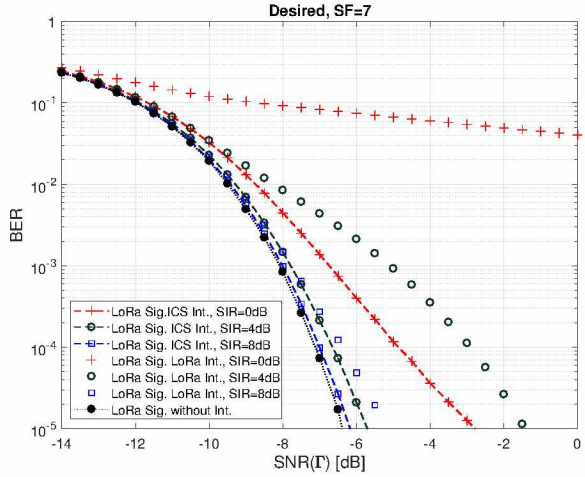

Fig. 5. Desired LoRa signal interfered by ICS-LoRa signal versus LoRa interfered by LoRa with $f = 7$.

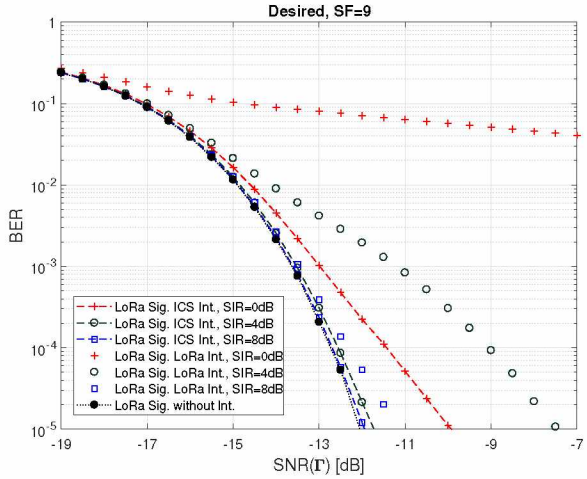

Fig. 6. Desired LoRa signal interfered by ICS-LoRa signal versus LoRa interfered by LoRa with $f = 9$.

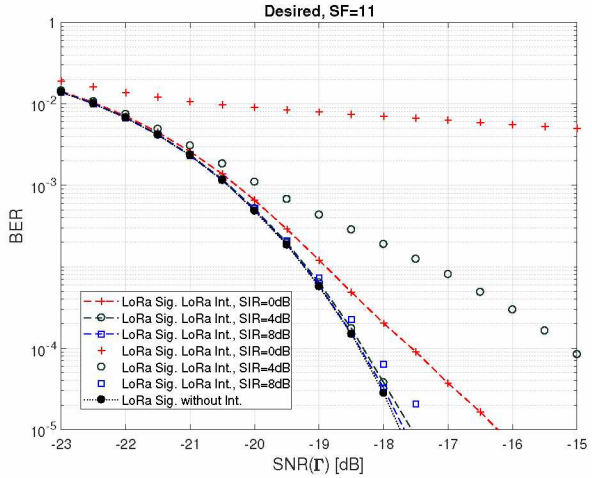

Fig. 7. Desired LoRa signal interfered by ICS-LoRa signal versus LoRa interfered by LoRa with $f = 11$.

C. BER Performance of ICS-LoRa due to Interference Cancellation

After the LoRa desired signal has been detected, the ICS-LoRa interferer signal has been also demodulated and detected according to the system block diagram in Figure 3. Figures 8, 9, and 10 show the BER performance of the ICS-LoRa interferer signal for SIR $\gamma = 0, 4, 8dB$ and for spreading factors $f = 7, 9, 11$ respectively. It can be easily noticed that at high SIR values, the interferer signal becomes noise-limited and so its BER performance is very much near that of the non-interfered signal performance. This is attributed to the interference cancellation technique considered in this paper where the interferer signal is decoded after the desired signal has been extracted from the aggregate received signal. Thus, the interferer signal becomes virtually interference-free. In such case the desired signal is detected with high reliability and so it is almost completely removed from the received signal. Therefore the residue of the signal is composed of the interferer signal with AWGN noise. This interference cancellation is more feasible in case LoRa interfered by ICS-LoRa, while in case of LoRa interfered by LoRa, this cancellation becomes harder to be achieved correctly since the desired signal will not be decoded with high reliability.

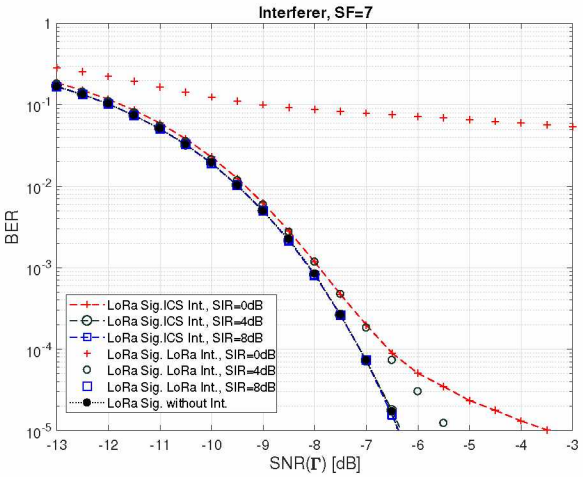

Fig. 8. Interferer signal for ICS-LoRa interference on LoRa signal versus LoRa interference on LoRa signal, with $f = 7$.

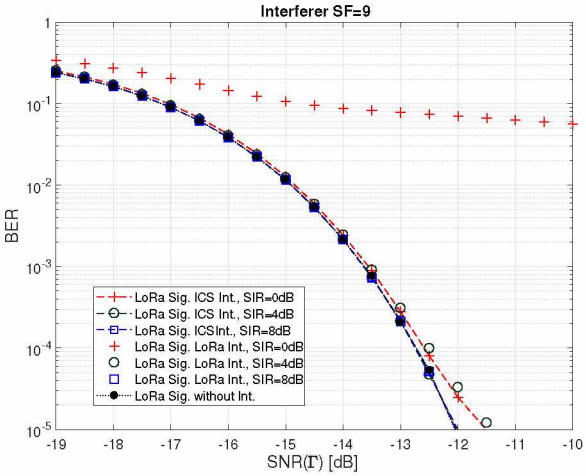

Fig. 9. Interferer signal for ICS-LoRa interference on LoRa signal versus LoRa interference on LoRa signal, with $f = 9$.

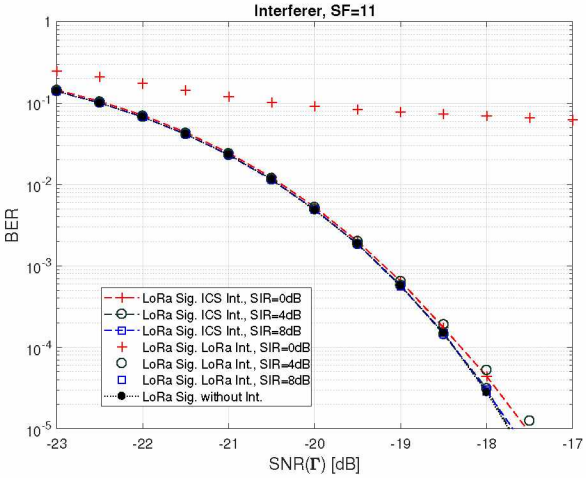

Fig. 10. Interferer signal for ICS-LoRa interference on LoRa signal versus LoRa interference on LoRa signal, with $f = 11$.

D. Coverage Regions

The curves in Figures 11 and 12 can be used to identify the coverage regions that reflect the joint impact of operating SNR Γ and SIR γ of both the desired LoRa signal and the interferer ICS-LoRa signal using the same f. These threshold SNR Γ_{th} values are considered to ensure coverage in the respective

LoRa logical network at a BER performance of 10^{-5}. It is evident from these Figures that at high values of SIR γ, the BER performance approaches that of the LoRa signal with no interference.

It can be noticed from Figures 11 and 12 that the performance loss is minimal between the signal LoRa and the interferer ICS-LoRa. The maximum loss is approximately $1.6dB$ in case of $f = 7$ and SIR $\gamma = 1dB$, while it is $3dB$ in case of $f = 11$ and SIR $\gamma = -2dB$. At SIR $\gamma = 6dB$, the performance loss is almost negligible.

Moreover, the coverage regions curves show the threshold Γ_{th} values at negative SIR γ values in case of ICS-LoRa interference. This is interpreted as decoding first the weaker signal. In this case, the decoder can still decode both interfering signals. Nevertheless, the receiver is most probably captured by the stronger signal to be decoded first, thus we will end up with the same system performance of the corresponding positive SIR γ value.

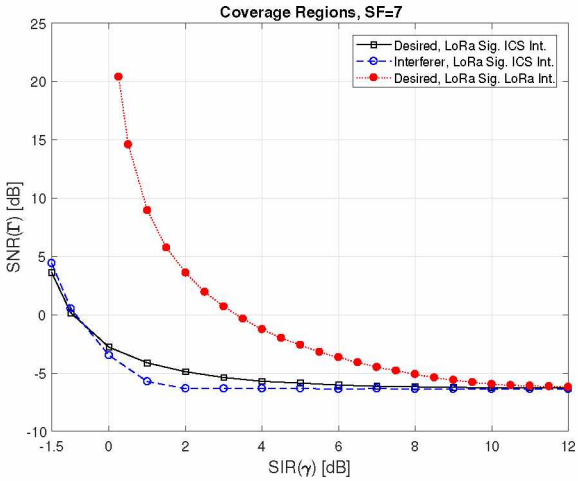

Fig. 11. Coverage Region of the Desired and Interferer signals, with $f = 7$.

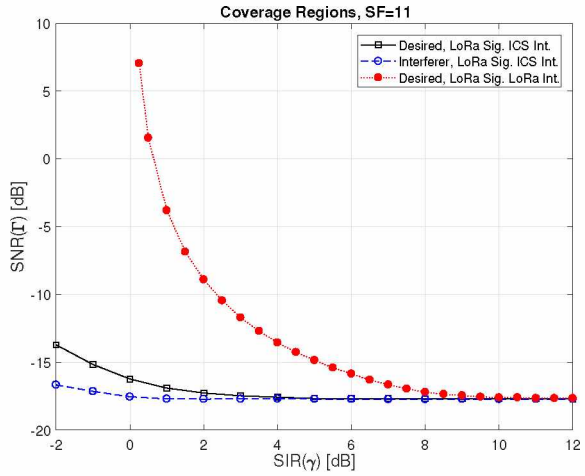

Fig. 12. Coverage Region of the Desired and Interferer signals, with $f = 11$.

V. Conclusions

In this paper, the ICS-LoRa is deployed as a new overlapping logical network that co-exists with the nominal LoRa network. The inter-network interference effect between the ICS-LoRa and the nominal LoRa logical networks are investigated and compared to the intra-network interference in case of concurrent nominal LoRa transmissions. Simulation results show that the ICS-LoRa interference has mild effects on the BER performance of nominal LoRa demodulation and vice versa. For spreading factor $f = 7$ and SIR value $\gamma = 4dB$, the LoRa signal interfered by ICS-LoRa has a BER degradation of approximately $0.7dB$ compared to $5dB$ in case of nominal LoRa interference. Moreover, for high SIR values the LoRa signal BER performance becomes noise limited and thus approaches the non-interfered signal performance. The interference cancellation is more feasible in case of the ICS-LoRa interference compared to the nominal LoRa interference since the stronger signal can be removed from the received signal with high reliability. Furthermore, for negative values of SIR, the receiver is still able to decode both interfering signals with good quality. Thus the overall system capacity is increased by utilizing ICS-LoRa together with the nominal LoRa system.

For future work, the LoRa and ICS-LoRa could be implemented and tested on a software-defined radio (SDR) platform in order to further validate their co-existence over real wireless channel and obtain more practical and reliable results. Moreover, the BER performance of the LoRa signal contaminated by ICS-LoRa interference could be numerically obtained and validated via the simulations done in this paper.

References

[1] O. Georgiou and U. Raza, "Low power wide area network analysis: Can lora scale?" *IEEE Wireless Commun. Lett.*, vol. 6, no. 2, pp. 162–165, April 2017.

[2] J. T. Lim and Y. Han, "Spreading factor allocation for massive connectivity in lora systems," *IEEE Commun. Lett.*, vol. 22, no. 4, pp. 800–803, April 2018.

[3] C. Goursaud and J.-M. Gorce, "Dedicated networks for IoT: PHY/MAC state of the art and challenges," *EAI endorsed transactions on Internet of Things*, Oct. 2015.

[4] D. Croce, M. Gucciardo, S. Mangione, G. Santaromita, and I. Tinnirello, "Impact of lora imperfect orthogonality: Analysis of link-level performance," *IEEE Commun. Lett.*, vol. 22, no. 4, pp. 796–799, April 2018.

[5] D. Bankov, E. Khorov, and A. Lyakhov, "Mathematical model of lorawan channel access with capture effect," in *2017 IEEE 28th Annual International Symposium on Personal, Indoor, and Mobile Radio Communications (PIMRC)*, Oct 2017, pp. 1–5.

[6] L. Feltrin, C. Buratti, E. Vinciarelli, R. D. Bonis, and R. Verdone, "Lorawan: Evaluation of link- and system-level performance," *IEEE Internet Things J.*, vol. 5, no. 3, pp. 2249–2258, June 2018.

[7] U. Noreen, L. Clavier, and A. Bounceur, "Lora-like css-based phy layer, capture effect and serial interference cancellation," in *European Wireless 2018; 24th European Wireless Conference*, May 2018, pp. 1–6.

[8] T. Elshabrawy and J. Robert, "Analysis of ber and coverage performance of lora modulation under same spreading factor interference," in *2018 IEEE 29th Annual International Symposium on Personal, Indoor and Mobile Radio Communications (PIMRC)*, Sep. 2018, pp. 1–6.

[9] N. E. Rachkidy, A. Guitton, and M. Kaneko, "Decoding superposed lora signals," in *2018 IEEE 43rd Conference on Local Computer Networks (LCN)*, Oct 2018, pp. 184–190.

[10] M. Hessar, A. Najafi, and S. Gollakota, "Netscatter: Enabling large-scale backscatter networks," *arXiv preprint arXiv:1808.05195*, 2018.

[11] T. Elshabrawy and J. Robert, "Interleaved chirp spreading lora-based modulation," *IEEE Internet of Things Journal*, pp. 1–1, 2019.

[12] L. Vangelista, "Frequency shift chirp modulation: The LoRa modulation," *IEEE Signal Process. Lett.*, vol. 24, no. 12, pp. 1818–1821, 2017.